Bulgarian Chemical Communications, Volume 53, Issue 1 (pp. 83 - 90) 2021 *DOI: 10.34049/bcc.53.1.5324*

Photocatalytic degradation of xylene cyanol FF dye using synthesized bismuth-doped zinc oxide nanocatalyst

F. Akbar Jan[1]*, U. Shah[1], M. Saleem[1], R. Ullah[1], N. Ullah[2], M. Usman[3], Sh. Hameed[1]

[1]*Department of Chemistry, Bacha Khan University Chrasadda, Khyber-Pakhtunkhwa,24420 Pakistan*
[2]*Department of Chemistry, Qauid-i-Azam University Islamabad, 45320 Pakistan*
[3]*Center for Research Excellence in Nanotechnology, King Fahd University of Petroleum and Minerals, Dhahran 31261, Saudi Arabia*

Received: August 28, 2020; Revised: October 14, 2020

Bismuth-doped zinc oxide nanoparticles were prepared through precipitation method. The synthesized nanoparticles were characterized by UV-Vis spectroscopy, Fourier transform infrared spectroscopy (FTIR), energy dispersive X-ray analysis (EDX) and high resolution-scanning electron microscopy (HR-SEM). The photo catalytic activity of the synthesized Bi-doped ZnO nanoparticles was evaluated in the photo degradation of xylene cyanol FF dye under UV-light. The effect of various reaction parameters like time, concentration, catalyst dosage, pH and temperature was also evaluated. Successful doping with bismuth reduced the band gap of zinc oxide from 3.25 eV to 2.9 eV. SEM study revealed that the synthesized nanoparticles have elongated morphology. From XRD the average crystallite size of Bi-doped ZnO was calculated to be 37 nm. At a duration of 120 min and low dye concentration (10 ppm) 67% degradation of the dye was achieved. Using an optimum catalyst dose (0.05 g) the degradation increased to 94% at pH 4. An increase in temperature decreased the rate of degradation and low temperature (15^{o}C) is considered to be favorable for the best degradation of xylene cyanol FF dye.

Keywords: Bi-doped zinc oxide nanoparticles, xylene cyanol FF dye, photocatalytic degradation, characterization

INTRODUCTION

Water pollution caused by industrialization, growing population, and consumerism has become severe in recent years [1-3]. Textile and dyeing industries are the major sources of pollution of surface and underground water [4-6]. Presence of a number of organic compounds including dyes in the drainage effluents from various industries creates environmental problems. These organic compounds are not easily decolorized by the conventional water treatment methods such as adsorption, biological treatment and coagulation [7]. The dyes are the most important constituent of emulsifiers, cosmetics, stabilizers, viscosity enhancing agents, antioxidants, lubricating substances and moisturizing agents [8, 9].

According to literature about 10,000 tons of dyes are produced *per annum*. Approximately 12 % of the total amount of dyes produced is lost during manufacturing and processing operations [10]. Dye exposure or inhalation can cause problems of respiratory and immune system, itching, watery eyes, sneezing, asthma, coughing and wheezing [11]. Free aromatic amines have been found to be formed during metabolism at the intestinal wall and in the liver, that are potentially carcinogenic and mutagenic [12, 13]. Exposure to azo group containing dyes can cause bladder cancer in humans (hepatocarcinomas) and nuclear anomalies in experimental animals and chromosomal aberration in mammalian cells [14]. Some dyes are causing phototoxic or photo allergic reactions. Contact dermatitis may result when substances on the skin are exposed to ultraviolet light [15]. One of the most commonly used dye is xylene cyanol FF which is used in textile industry and as a laboratory substance for the spectrophotometric determination of amines, trace nitrite and aniline. The leuco xylene cyanol FF form (LXCFF) is used for the determination of trace quantities of gold, Cr (VI), iron and aluminum in ores and rocks [16]. It is an anionic compound which mediates the electron/proton transfer reaction easily on the carbon paste electrode. It also has an electron-rich oxygen group ($–SO^{3–}$) in its structure. These negatively charged $–SO^{3–}$ groups on the electrode surface have high affinity towards the positively charged analyte in the solution and produce high current signals with L-dopa [17]. Conventional waste water treatment methods such as coagulation, reverse osmosis, ion exchange, ozonation, flocculation, activated carbon adsorption are ineffective due to high operating cost and production of a large volume of sludge.

* To whom all correspondence should be sent:
E-mail: fazal_akbarchem@yahoo.com

Owing to its economy and abundance of the materials photo catalysis using semiconductors has been recommended as a potential method for environmental clean-up. These methods degrade pollutants by using artificial or natural photons. No formation of sludge and catalyst regeneration are among the advantages of using photo catalysis [18]. Due to the wide band gap energy of 3.37 eV (bulk), harmless nature and high photosensitivity ZnO is generally considered as a good photo catalyst for the degradation of organic dyes. Electron-hole recombination rate is the only drawback of ZnO which reduces the degradation efficiency. For enhancing its activity many researchers reported doping of ZnO with impurity atoms [19]. The photo catalytic properties of ZnO could be enhanced by many transition metals such as Mn, Cu and Co or rare earth elements (La, Ce and Er) [20].

Keeping in view the benefits of photo catalysis it offers over other conventional treatment methods a study was designed to synthesize and characterize bismuth=doped zinc oxide nanoparticles and to apply them as a catalyst for the photo catalysis of xylene cyanol FF in aqueous medium.

EXPERIMENTAL

Instruments

UV-Vis spectrophotometer model Shimadzu UV-1800, Japan was used for all absorbance measurements. Perkin Elmer FTIR spectrometer version 10.4.00 was used for identification of functional groups. Elico (model IL-610) digital pH meter was used for pH measurements. Morphology and elemental composition of the doped nanoparticles was investigated using a SEM-EDX JEOL 5600LV microscope at an accelerating voltage up to 30 kV at the Center for Research Excellence in Nanotechnology, King Fahd University of Petroleum and Minerals, Dhahran, Saudi Arabia.

Reagents

Analytical grade reagents such as bismuth nitrate pentahydrate, zinc acetate, xylene cyanol FF dye, oxalic acid and nitric acid were purchased from Sigma Aldrich. For ensuring freedom of contamination all glass ware was rinsed with double distilled water.

Preparation of Bi-doped ZnO nanoparticles

Precipitation method was used for the preparation of Bi-doped ZnO nanoparticles. A calculated amount of $Bi(NO_3)_2.5H_2O$ was dissolved in 0.2M HNO_3 solution. Constant amounts of oxalic acid and zinc acetate dihydrate were also dissolved in distilled water. Oxalic acid-to-zinc acetate dihydrate atomic ratio was 0.8 at the doping ratio Bi/ZnO of 5.0. At room temperature and under vigorous stirring bismuth nitrate pentahydrate solution was added dropwise into the zinc acetate dihydrate solution until the formation of precipitate. The resulting precipitate was then thoroughly washed with double distilled water to remove the anions. The resulted precipitate was dried in an oven at 100°**C** for 12 hours followed by calcination in a furnace at 600°C for 3 hours.

Preparation of dye solution

Stock solution (500 ppm) of xylene cyanol FF dye was prepared by dissolving 0.125 g of dye in distilled water. Then working solutions of different concentrations were prepared using the following dilution formula (Eq. 1):

$$C_1V_1=C_2V_2 \quad (1)$$

Procedure for photo catalytic degradation

First of all the absorbance of the original xylene cyanol FF solution was recorded and maximum absorption was found at 614 nm. This was recorded as a monitor wavelength for all the measurements. Appropriate amounts of photo catalyst, i.e bismuth-doped ZnO were separately added to working solutions. The mixed solution was stirred for 30 min in dark to establish adsorption/desorption equilibrium before the photo degradation reaction. The dispersions were kept in light source. During experiments a UV lamp with the power of 1500 watts was placed 15 cm away from the surface of the solution in a locally designed equipment. The dye degradation was checked at various intervals of time and the catalyst was removed by centrifugation. The absorbance of the centrifuged solution was measured on a UV-Vis spectrometer. The percent photo degradation of xylene cyanol FF was calculated by using the following relation (Eq. 2):

$$D\% = \frac{C_o - C_1}{C_o} x100 \quad (2)$$

where C_0 and C denote the concentrations of xylene cyanol FF at time 0 min and t (s), respectively, and t is the irradiation time.

RESULTS AND DISCUSSION

Characterization of the catalyst (Bi-doped ZnO nanoparticles)

UV–Vis studies. The UV-Vis spectra of undoped ZnO and Bi-doped ZnO nanoparticles are shown in Fig. 1.

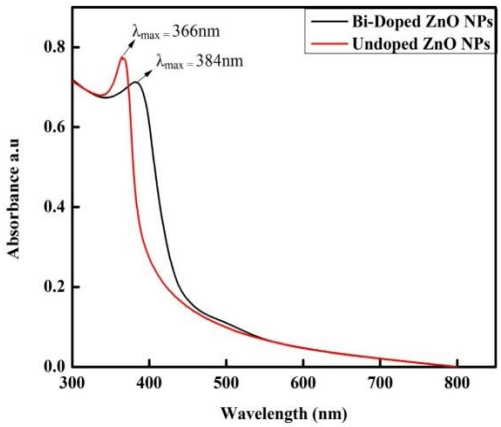

Fig. 1. UV-Vis spectra of undoped and Bi-doped ZnO NPs.

The characteristic absorption peak of undoped ZnO occurs at 366 nm and that of Bi-doped ZnO nanoparticles appears at 384 nm. From the spectra it can be seen that the maximum absorption of doped-ZnO nanoparticles is shifted towards the higher wavelengths, i.e. demonstrated a bathochromic shift as compared with undoped ZnO NPs and also band edge was red shifted [21].

The band gap was calculated using the following relation (Eq. 3):

$$\alpha h\upsilon = A(h\upsilon - Eg)^n \quad (3)$$

where α is the absorption coefficient, hυ represents the energy of photon, A is proportionality constant, it is different for different materials while n represents the index. From the graph the optical band gaps of undoped ZnO and Bi- doped ZnO were calculated which came out to be 3.25 eV and 2.9 eV, respectively, as shown in Fig. 2. They are closely related to the literature value [22].

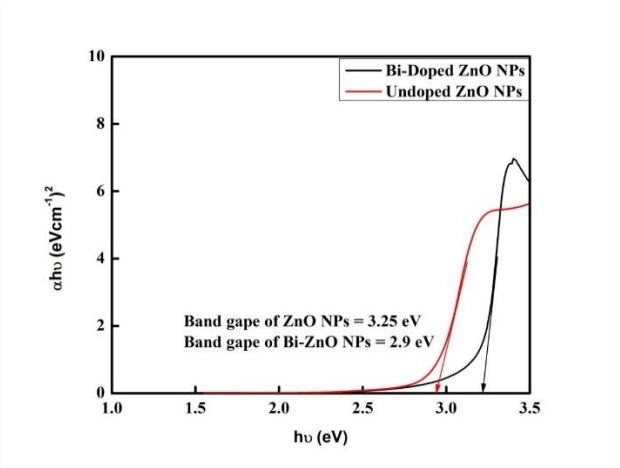

Fig. 2. Energy gap of undoped and Bi-doped ZnO NPs

XRD studies. XRD patterns of undoped ZnO and Bi-doped ZnO NPs are shown in Fig. 3. According to JCPDS card number 36-1451 all the diffraction peaks were related to the hexagonal wurtzite structure of undoped ZnO. In case of Bi-doped ZnO NPs additional small peaks star-marked at 2 theta of 27.89, 32.69, 56.22 and 55.47 were ascribed to the Bi_2O_3 peaks according to JCPDS card No. 712274 and 501088.This shows the minor phase of Bi_2O_3 as compared to ZnO major phase. From the pattern it can also be seen that due to Bi doping the intensity of the major peaks decreases. Debye-Scherrer equation was used to calculate the average crystallite size of undoped ZnO and Bi-doped ZnO nanoparticles:

$$L = K\lambda/\beta\cos\theta \quad (4)$$

where L is an average crystalline site, K represents a dimensionless factor relating to shape having a value of 0.9, λ shows the wavelength of the X-rays, β is the Full width half maximum (FWHM) in radians and θ represents Bragg angle. The average crystalline size of undoped and Bi-doped ZnO NPs comes out to be 23 and 37 nm, respectively.

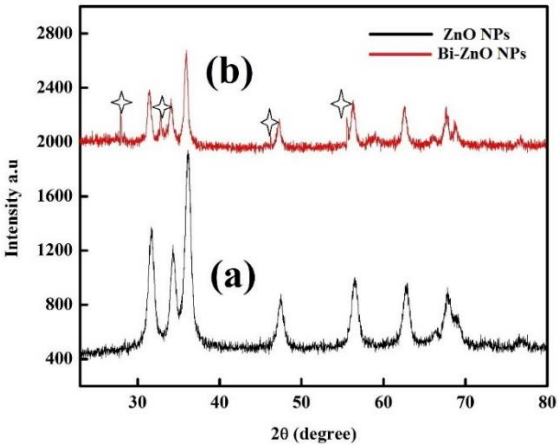

Fig. 3. X-ray diffraction patterns of **(a)** undoped ZnO and **(b)** Bi-doped ZnO.

SEM with EDX analysis. The SEM image given in Fig. 4 shows a collection of elongated particles of various plate-like shapes [23]. The average size of the particles is 2 μm. Energy dispersive X-ray spectroscopy was used for determining the elemental composition of Bi-doped ZnO nanoparticles as shown in Fig. 5. The EDX spectrum indicates the presence of Zn, O and Bi as major elements and gives the quantitative measurement of weight percentage of compositional elements. The elemental composition and weight percentage of the elements are summarized in Table 1 [24].

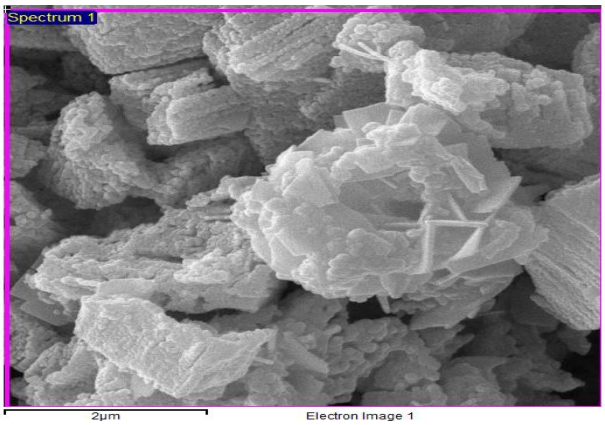

Fig. 4. SEM image of Bi doped-ZnO nanoparticles

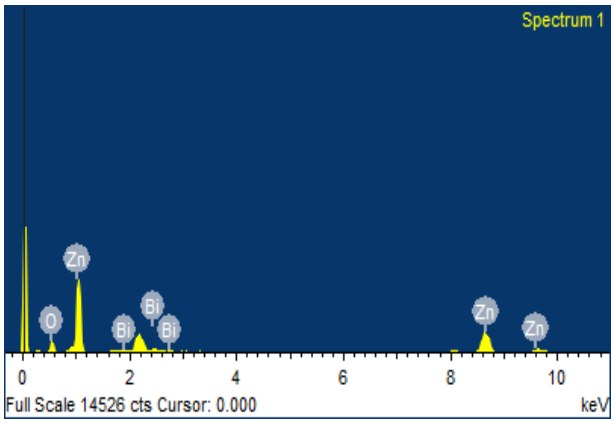

Fig. 5. EDX spectrum of Bi-doped ZnO nanoparticles

Table 1. Elemental composition of Bi-doped ZnO nanoparticles

Element	Weight %	Atomic %
O K	18.47	50.64
Zn K	69.91	46.92
Bi M	11.62	2.44
Totals	100.00	

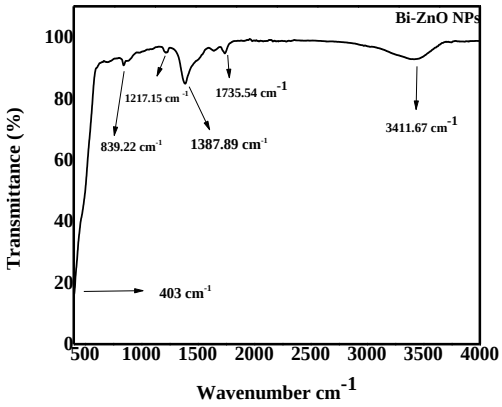

Fig. 6. FTIR spectrum of Bi-doped ZnO nanoparticles

Photo catalytic degradation of xylene cyanol FF dye

Effect of contact time on dye degradation. In order to study the effect of contact time on the degradation of xylene cyanol FF dye, 30 mL of the dye solution was taken in a beaker and 0.02 g of Bi doped-ZnO catalyst was added and kept in dark for 20 min. Then the mixture was irradiated by UV light for the time intervals of 20, 40, 60, 75, 90, 105, 115 and 125 min. Fig. 7 shows the changes recorded in the UV spectrum at various intervals of time during the experiment. Initially, at 20 min time duration the degradation was very low (6%) with an increase in time duration the degradation also increased as shown in Table 2. Increasing the time duration up to 120 min the degradation exponentially increased and about 67% of the dye was degraded. Time interval of 125 min was recorded as the optimum time for the degradation of the dye. This can be attributed to the fact that initially the photo catalyst surface is exposed to the light photons and with the passage of time the catalyst surface gets saturated by the adsorption of dye molecules, as a result the relative number of OH• needed for the dye molecules decreases, which eventually claims the photo catalyst activity [29].

Table 2. Effect of time on the dye degradation

Time (min)	20	40	60	75	90	105	115	120
Degradation (%)	6	12.5	45	49	54	61	65	67

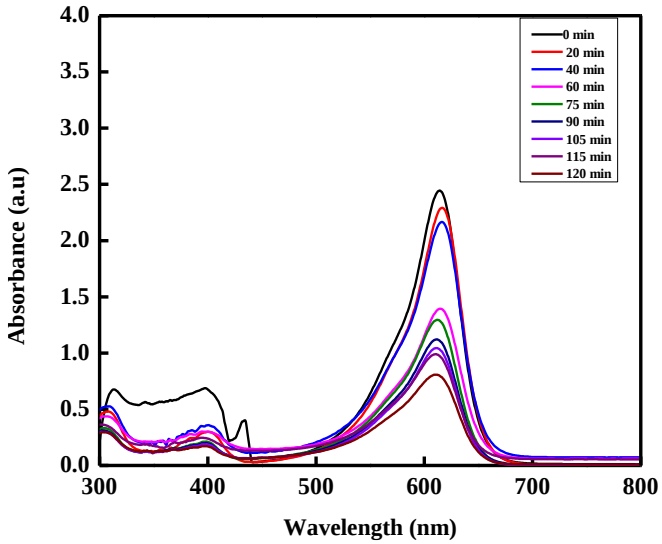

Fig. 7. Effect of time on dye degradation using Bi-doped zinc oxide NPs.

Table 3. Effect of dye concentration on the degradation

Initial concentration of the dye (ppm)	10	20	30	40	50	60	70
Degradation (%)	66	56	37	29	20	16	9.3

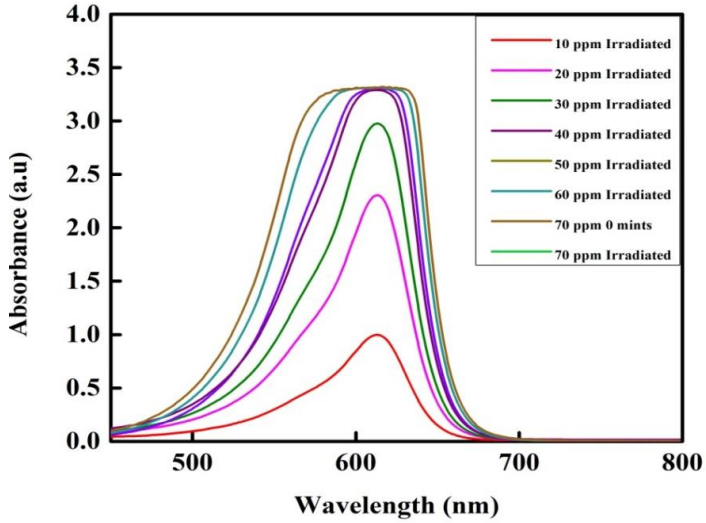

Fig. 8. Effect of concentration on dye degradation using Bi-doped zinc oxide NPs

Effect of initial concentration on the dye degradation. The concentration has an immense effect on the degradation of dye. Solutions of different concentrations ranging from 10 ppm to 90 ppm were prepared in 30 mL of distilled water. Then 0.02 g of the catalyst was added to each solution and placed under UV light for time duration of 120 min. Initially, at 10 ppm high percentage of degradation of xylene cyanol FF was recorded (Table 3) which eventually decreased with an increase in the concentration of dye solution. Fig. 8 depicts the changes in the rate of degradation of xylene cyanol FF dye with increase in dye concentration. It is because as the dye concentration increases, more dye molecules get adsorbed on the photo catalyst surface and shield the catalyst surface from light photons which in turn reduces the path length of the photons entering the dye solution [30, 31]. This is also a reason that can explain that increased dye concentration saturates the photo catalyst surface and the requirement of catalyst for the process also

increases. Keeping the irradiation time and catalyst loading constant, the $OH^{\cdot}$ radical formation on the surface of the semiconductor also becomes constant. That is why on increasing dye concentration the relative number of OH• needed for the dye molecules decreases [32].

Effect of dosage rate on dye degradation. Dosage of the catalyst may also affect the rate of degradation. For studying the effect of dosage rate on dye degradation, a working solution of 10 ppm was prepared in 250 mL of distilled water. Then 5 mL was taken from the original solution. Dosage of catalyst ranging from 0.01 to 0.07 g was used during experiments. The degradation at different dosage rates was recorded. Table 4 shows that initially, at a low dose of the catalyst (0.01 g) the degradation was 5.8% only which hiked to 37%, 40%, 52% and 86% upon increasing the dose rate from 0.01 to 0.05 g. On further increasing of the amount of catalyst beyond 0.05 g the degradation declined to 53% at 0.06 g and to 15% at 0.07 g. The rate of degradation increased with catalyst loading till certain weight and above this the rate of degradation of the dye decreased with increase in weight as reported by many researchers. This is not unusual because in solution phase reactions the exposed surface area of the catalyst will not be directly proportional to the amount of catalyst loaded. Since the amount that is adsorbed on the surface of the solid dye degradation is proportional to that and there can be a saturation point beyond which the solid amount may not have a direct relationship to the degradation extent. Maximum amount of the solid loaded for maximum activity is 3-4 g per liter of the dye solution as reported by studies [33]. The change in the degradation rate with increase in dosage rate is shown in Fig. 9.

Effect of pH on the dye degradation. The pH also has a strong effect on the dye degradation. The pH of the original solution of xylene cyanol FF dye was checked by the pH meter. The pH of xylene cyanol FF solution was 6.39, near to neutral. Then 20 ppm of the dye solution were added to 250 mL of distilled water. Then solutions of different pH were prepared by using 0.1 N NaOH and 0.1 N HCl. The pH was adjusted in the range from 4 to 10. An optimum weight of the catalyst (0.05 g) was added to each solution. Table 5 shows that at pH 4 high degradation (94%) was found while at pH 5 the degradation was 4.9% only. The effect of pH on dye degradation is shown in Fig. 10. For the photo catalytic degradation process adsorption of dye is an essential step. Faster will degrade the dye which has a high adsorption capacity. The concentration of hydroxyl radicals and adsorption on photo catalyst will determine the extent of degradation. Activity of ions (e.g. H+ or pH) determines the potential of the surface charge in photo catalyst/aqueous systems. The property of a surface to become either positively or negatively charged is a function of pH. Maximum degradation of xylene cyanol FF was observed in acidic medium in our study [34].

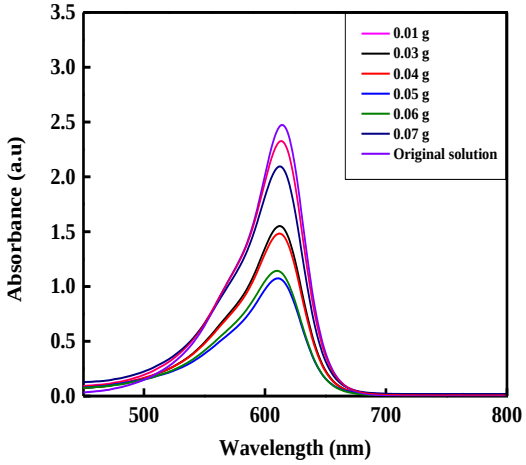

Fig. 9. Effect of dosage rate on dye degradation using Bi-doped zinc oxide NPs

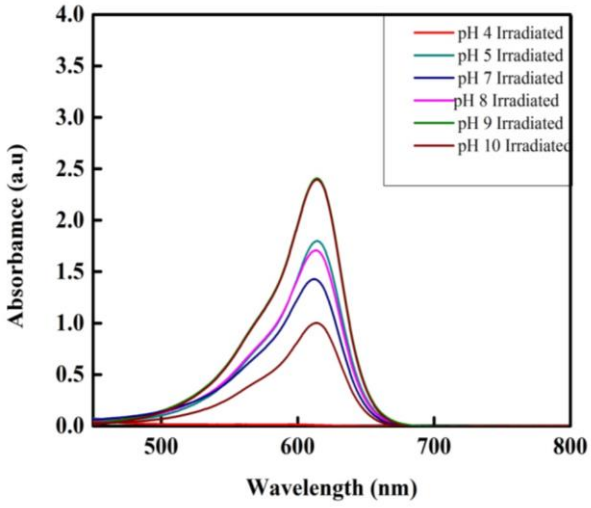

Fig. 10. Effect of pH on dye degradation using Bi-doped zinc oxide NPs.

Table 4. Effect of catalyst dosage on dye degradation

Catalyst mass (g)	0.01	0.02	0.03	0.04	0.05	0.06	0.07
Degradation (%)	5.8	37	40	52	86	53	15

Table 5. Effect of pH on dye degradation

pH value	4	5	7	8	9	10
Degradation (%)	94	4.9	6	5.2	6.4	5.6

Table 6. Effect of temperature on dye degradation

Temperature (°C)	15	25	35	45	55
Degradation (%)	82	62	37	22	15

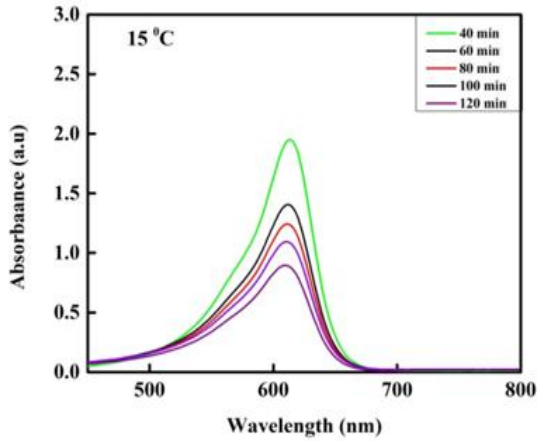

Fig. 11. Effect of temperature on dye degradation using Bi-doped zinc oxide NPs

Effect of temperature on dye degradation. Temperature also affects the degradation of dye. In order to establish the effect of the temperature on the dye degradation a solution of 20 ppm was prepared. Exactly 30 mL from the stock solution was taken in a beaker to which 0.05 g of Bi-doped ZnO nanoparticles were added. The temperature was kept at 15°C, 25°C, 35°C, 45°C, and 55°C, respectively. Maximum degradation (82%) was recorded at a temperature of 15°C at 120 min time interval while the degradation at 25°C, 35°C, 45°C and 55°C was not appreciable. The effect of temperature on the degradation is shown in Fig 11 and Table 6. It can be seen that at 15°C best percent degradation was observed. It can be attributed to the fact that an increase in temperature leads to the evaporation of the solvent, as a result percent degradation in open environment decreases.

CONCLUSIONS

It can be concluded from the present study that doping of zinc oxide with bismuth effectively decreases the band gap of the nanoparticles. Synthesized bismuth doped-ZnO nanoparticles have elongated shapes and are shown as a collection of particles. The degradation of xylene cyanol FF increases with an increase in time duration. Low concentration (100 ppm) of the dye and an optimum weight of the catalyst (0.05 g) was found best for the photo catalytic degradation of xylene cyanol FF dye. The pH study revealed that at pH 4 maximum degradation (94%) of xylene cyanol FF was noticed. Increase in temperature leads to evaporation of the dye solution and best degradation was noticed at 15°C temperature. Bismuth-doped zinc oxide catalyst can be effectively used for the degradation of xylene cyanol FF dye in waste water supplies.

Conflict of interest: *The authors declare no conflict of interest for this publication.*

REFERENCES

1. A. Minelgite, G. Liobikiene, *Sci. Tot. Environ.*, **672**, 174 (2019).
2. R. T. Kant, *Nat. Sci.*, **4**, 22 (2012).
3. G. J. Nohynek, R. Fautz, F. Benech-Kieffr, H. Toutain, *Food and Chem. Toxicol.*, **42**, 517 (2014).
4. S. Gita, A. Hussan, T. G. Choudry, *Environ. Ecol.*, **35**, 2349 (2017).
5. F. I. Vacchi, A. F. Albuquerque, J. A. D. A. Vendemiatti, Morales, A. B. Ormond, H. S. Freeman, G. Umbuzeiro, *Sci. Tot. Environ.*, **2**, 302 (2013).
6. D. Oliveira, A. R. Gisele, D. L. Joaquin, T. C. P. Elisabet, B. Miquel, D. Danielle, O. Palma, *Environ. Toxicol. Chem.*, **35**, 429 (2016).
7. W. A. Żukiewicz-Sobczak, P. Adamczuk, P. Wroblewska, J. Zwolinski, J. Chmielewska-Badora, E. Krasowska, J. Kozlik, *Adv. Dermatol. Allerg.*, **30**, 307 (2013).
8. A. R. Ribeiro, G. Arangaoumbuzeiro, *Environ. Sci. Eur.*, **26**, 22 (2014).
9. J. Sima, P. Hasal, *Chem. Eng.*, **32**, 79 (2013).
10. M. A. Hassan, A. El Nemr, F. F. Madkour, *Amer. J. Wat. Sci. Eng.*, **2**, 14 (2016).
11. E. A. Meulenkamp, *The J. Phys. Chem. B.*, **102**, 5566 (1998).
12. F. Akarsalan, H. Demiralay, *Acta. Physica Pol. A.*, **128**, 407 (2015).

13. T. Y. Lin, Y. T. Hsu, W. H. Lan, C. J. Huang, L. C. Chen, Y. H. Huang, K. F. Huang, *Adv. Nano. Res.*, **3**, 123 (2015).
14. B. S. Padhi, *Int. J. Environ. Sci.*, **3**, 940 (2012).
15. M. Pandurangachar, B. K. Swamy, U. Chandra, O. Gilbert, B. S. Sherigara, *Int. J. Electrochem. Sci.*, **4**, 672 (2009).
16. L. Cai, C. Xu, *J Braz. Chem. Soc.*, **22***(*10), 1823 (2011).
17. L. A. Chanu, W. J. Singh, K. J. Singh, K. N. Devi, *Results in Phys.*, **12**, 1230 (2019).
18. V. L. Chandraboss, L. Natanapatham, B. Karthikevan, J. Kamalakkanan, S. Prabha, S. Senthilvelan, *Mat. Res. Bull.*, **48**, 3707 (2013).
19. E. F. Keskenler, S. Aydin, G. Turgut, S. Dogan, *Acta Physica Polonica, A*, **126**, 3 (2014).
20. T. Prakash, G. Neri, A. Bonavita, E. R. Kumar, K. Gnanmoorthi, *J. Mat. Sci. Mater. Electron.*, **26**, 4913 (2015).
21. K. Handore, S. Bhavsar, A. Horne, P. Chhattise, K. Mohite, J. Ambekar, V. J. Chabukswar, *Macromolec. Sci.* A, **51**, 941 (2014).
22. H. Barrak, T. Saied, P. Chevallier, G. Laroche, A. Mnif, A. H. Hamzaoui, *Arab. J. Chem.*, DOI:http//dx.doi.org/10.1016/j.arabjc.2016.04.019
23. R. N. Moussawi, D. Patra, *RSC Adv.*, **6**, 17256 (2016).
24. M. K. Trivedi, R. M. Tallapragada, A. Branton, D. Trivedi, G. Nayak, O. Latiyal, S. Jana, *Am. J. Nan. Res. Appl.*, **3**, 94 (2015).
25. A. Kumar, G. Pandey, *Mater. Sci. Eng. Int. J.*, 106 (2017).
26. N. Daneshvar, D. Salari, A. R. Khataee, *J. Photochem. Photobiol.*, **162**, 317 (2004).
27. E. M. Saggioro, A. S. Oliveira, T. Pavesi, C. G. Maia, L. F. V. Ferreira, J. C. Moreira, *Molecules*, **16**, 10370 (2011) .
28. Z. Mengyue, C. Shifu, T. Yaowu, *J. Chem. Technol. Biot.*, **64,** 339 (1995).
29. B. Viswanathan, *Curr. Cat.*, **7**, 99 (2018).
30. V. L. Chandrabos, J. Kamalkkannan, S. Prabah, S. Senthilvelan, *RSC Adv.*, **5**, 25857 (2015).
31. M. A. Hassaan, A. El Nemr, *Am. J. Environ. Sci. Eng.*, **1**, 64 (2017).
32. X. Li, Y. Hou, Q. Zhao Wang, *J. Colloid Interf. Sci.* **358**, 102 (2011).
33. U. G. Akpan, B. H. Hameed, *J. Hazard. Mater.*, **170**, 520 (2009).
34. F. Zhang, J. Zhao, T. Shan, H. Hidaka, E. Pelizzetti, N. Serpone, *Appl. Catalysis B-Environ.*, **15**, 147 (1998).